

Optimization and Mechanistic Insights for Methyl Orange Adsorption Using Na₂CO₃ Activated Puffed Rice Biochar

Muhammad Saidur Rahman^{a*}, Aneek Krishna Karmakar^b and Fahima Khatun^b

^aPundra University of Science and Technology, Gokul, Bogura-5800, Bangladesh

^bApplied Chemistry and Chemical Engineering, University of Rajshahi, Rajshahi- 6205, Bangladesh

(received March 20, 2024; revised October 22, 2024; accepted October 23, 2024)

Abstract. This research investigated the efficient removal of methyl orange (MO) from water sources through the utilization of activated carbons derived from puffed rice and activated with Na₂CO₃. Several operational parameters, including shaking time, biochar particle sizes, MO concentration, Na₂CO₃ concentration and temperature were examined. The size of particles plays a crucial role in MO adsorption due to the increased surface area of biochar. Experimental results demonstrate that puffed rice biochar exhibits remarkable adsorption capacity for MO, achieving an adsorption capacity of 0.588 mg/g and approximately 99% removal efficiency with a sample weight of 1 g, Na₂CO₃ concentration of 1 mol/L, initial MO concentration of 29.599 mg/L, particle size of 170 μm, temperature of 303 K and 20 mL volume of MO solution and a shaking time of 60 min. Analytical techniques such as FTIR, SEM imaging and XRD spectroscopy were employed for substance analysis. SEM analysis of Na₂CO₃ activated puffed rice biochar showed a highly porous structure, enhancing its adsorption capacity. XRD confirmed its amorphous nature, making it effective for removing contaminants like methyl orange. The FTIR spectra suggest a complicated composition, with peaks for aliphatic hydrocarbons and possible halogenated chemicals. After introducing methyl orange (MO), variations in the spectrum indicate interactions with the biochar's functional groups while retaining structural stability. Hence, improving dye adsorption capacity the adsorption isotherm study supported the Langmuir model, suggesting monolayer adsorption behaviour, however greater MO concentrations lowered adsorption effectiveness. Thermodynamic analysis indicates that the process is exergonic, non-spontaneous and has positive ΔG° values. The FTIR spectra suggest a complicated composition with peaks for aliphatic hydrocarbons and possible halogenated chemicals. After introducing methyl orange (MO), variations in the spectrum indicate interactions with the biochar's functional groups, while retaining structural stability, hence improving dye adsorption capacity. Adsorption isotherm study supported the Langmuir model, suggesting monolayer adsorption behaviour, however greater MO concentrations lowered adsorption effectiveness. Thermodynamic analysis indicates that the process is exergonic, non-spontaneous and has positive ΔG° values. Finally, Na₂CO₃ activated puffed rice biochar is an environmentally benign and cost-effective approach for removing MO colour from wastewater.

Keywords: adsorption, equilibrium, puffed rice biochar, Na₂CO₃ activated biochar, optimization, methyl orange dye, wastewater treatment

Introduction

Water, often described as the "elixir of life," is indispensable for sustaining all life forms on earth. It plays pivotal roles in various biological processes, regulating body temperature and facilitating cellular hydration, all vital for survival. Human activities and agricultural endeavors heavily rely on water, serving essential functions such as crop irrigation and meeting the hydration needs of communities worldwide (Azizullah *et al.*, 2011). However, water resources pose risks when mismanaged or contaminated. Various pollution sources, including resource extraction, oil spills, agricultural practices, nuclear waste leakage and industrial discharge, contribute

*Author for correspondence;

E-mail: saeed_hamim@yahoo.com

to the deterioration of water quality (Gao *et al.*, 2019; Ogemdi, 2019).

Bangladesh's economy relies heavily on agriculture, engaging approximately 48.4% of the population directly. Agriculture significantly contributes to the country's GDP, accounting for about 17.5% (FAO, 2020). With a population of 162.7 million and a high population density, Bangladesh faces challenges in meeting the increasing demands for food and energy. The government projects a population growth rate of 1.59%, with estimates suggesting the population could reach around 265 million by 2050. This anticipated increase further strains already limited resources such as land and forests (BBS, 2018; 2017).

The importance of biochar in wastewater treatment is substantial, as it effectively removes various contaminants including heavy metals, pesticides, pharmaceuticals, plasticizers, dyes, organic and inorganic materials. Biochar is formed through the pyrolysis of biomass at temperatures below 700 °C in the absence of oxygen (Park *et al.*, 2011). Metal contamination in wastewater poses a significant concern in several countries, including Turkey, China, India and Bangladesh, as evidenced by recent surveys (Hassan *et al.*, 2020).

Although biomass emissions match the amount of CO₂ emissions during conversion and utilization as in photosynthesis, biochar demonstrates promise as a sustainable, carbon neutral substance (Yuan *et al.*, 2019). Wastewater containing dyes is a byproduct of various human activities, such as those in the food, textile and pharmaceutical industries (Cui *et al.*, 2016). This wastewater presents significant challenges due to its carcinogenic, teratogenic and mutagenic properties, posing potential risks to human health and ecological balance (Torrades, 2014). MO is a commonly used azo dye in industries like printing and dyeing, noted for its resistance to decomposition, high chroma and poor biochemical purification capacity (Saleh and Gupta, 2012).

Adsorption stands as a widely embraced method for dye removal from wastewater, owing to its advantages such as flexibility, operational simplicity, minimal sludge volume and low setup costs (Selvasembian *et al.*, 2021; Gunarathne *et al.*, 2020; Adithya *et al.*, 2019). Nonetheless, drawbacks include the potential toxicity of wastes produced from spent adsorbents, the requirements for chemicals in desorption and the transfer of pollutant load rather than its complete elimination (Iwuozor *et al.*, 2021). The efficacy of adsorption significantly hinges on the properties of adsorbents, particularly their porosity and surface area. Activated carbon, a frequently utilized adsorbent, is renowned for its large pore size and high surface area (Demirbas *et al.*, 2008).

Pyrolysis, a process that yields biochar or "Black Gold," involves the creation of carbon rich biomass under high temperature and low oxygen conditions. By utilizing various waste biomasses such as rice husks, wood, bones and straw, biochar emerges as a promising soil amendment characterized by qualities such as low heat conductivity, high porosity, renewability, stability and substantial carbon content (Seow *et al.*, 2022).

Methyl orange (MO) is one of the most commonly used dyes in the textile industry, an anionic dye known for

its detrimental effects on aquatic environments and aesthetic value reduction when discharged into wastewater (Balarak *et al.*, 2016; Bazrafshan *et al.*, 2014; Mo *et al.*, 2008). Numerous methods have been developed to treat dye wastewater, including flocculation sedimentation, ion exchange, ultrafiltration, dialysis, chemical oxidation, photo-oxidation, electrolysis and adsorption (Zhang *et al.*, 2020; Jiang *et al.*, 2017; Li, 2017). Among these, adsorption stands out as a simple, cost-effective and environmentally friendly approach compared to others that can be expensive and generate harmful waste (Hassan *et al.*, 2020; Wang *et al.*, 2019).

The objective of this study is to assess the adsorption capacity of Na₂CO₃ activated puffed rice biochar for the removal of methyl orange from aqueous solutions. We also seek to optimize operational parameters such as shaking time, particle size, MO concentration, Na₂CO₃ concentration and temperature to maximize adsorption efficiency. This investigation further aims to provide mechanistic insights through structural and morphological characterization of the biochar using techniques such as SEM, FTIR and XRD. By elucidating the interactions between the biochar surface and dye molecules, this study contributes to the growing body of research on sustainable wastewater treatment and the potential of biochar as an effective adsorbent (Adithya *et al.*, 2019; Park *et al.*, 2011).

Materials and Method

Collection and production of puffed rice biochar.

Puffed rice was sourced from a local market and ground into a fine powder using a grinder. A clean, contaminant free muffle furnace was used to hold 5 g of the ground puffed rice biochar. Sodium carbonate (Na₂CO₃, purity: 99.5%, Sigma-Aldrich) was added to the puffed rice to activate the material. During pyrolysis, a vent was incorporated to allow for the release of gases, ensuring that the pyrolysis process remained controlled. The furnace temperature was set at 573 K (300 °C) and maintained for 1 h to produce biochar. After pyrolysis, the material was cooled and then sieved into two particle sizes: 120 µm and 170 µm using standard sieves (Retsch, Germany).

Preparations of different reagents. A stock solution of 0.1 mol/L HCl was prepared by diluting concentrated hydrochloric acid (HCl, 11.3 mol/L, 99.99% purity, Merck) with distilled water and it was used for the washing studies. A stock solution of methyl orange (MO, C₁₄H₁₄N₃NaO₃S, molecular weight: 327.33 g/mol,

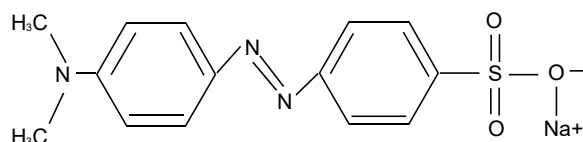


Fig. 1. The chemical formula of MO.

99.99% purity, Sigma-Aldrich) was prepared by dissolving 0.327 g of MO in 100 mL of distilled water, resulting in a concentration of 327 mg/L. Diluted concentrations of MO were prepared using distilled water as needed. Additionally, Na_2CO_3 stock solutions of 1 mol/L and 2 mol/L were prepared by dissolving 10.6 g and 21.2 g of Na_2CO_3 , respectively, in 100 mL of distilled water. The structural formula MO is depicted as in Fig. 1.

Analytical. Batch adsorption experiments were performed by mixing 20 mL of MO solution with various amounts of puffed rice biochar (0.5 g, 1 g and 1.5 g) in 220 mL reagent bottles. The mixtures were agitated at 300 strokes/min for 60 min using a mechanical shaker. For temperature dependent studies, a thermostatic water bath maintained at 303 ± 0.5 K (30°C) was used. After shaking, the solutions were filtered and the absorbance was measured using a UV-Vis spectrophotometer (Shimadzu UV-1800) at a wavelength of 462 nm to determine the remaining concentration of MO.

Preparation of Na_2CO_3 activated puffed rice biochar.

For the production of activated carbon, the biochar derived from puffed rice was further processed to enhance its adsorption properties. Puffed rice was first ground using a mortar and pestle. It was then subjected to a muffle furnace for 1 h at 573 K to achieve complete carbonization. The resulting activated carbon was prepared by impregnating the carbonized material overnight with different concentrations of Na_2CO_3 (1 mol/L, 2 mol/L, 3 mol/L and 4 mol/L) at a ratio of 1:5 (adsorbent). The impregnated samples were dried in an oven at 110°C for 8 h and then carbonized again at 300°C for 1 h.

After carbonization, the samples were neutralized by washing with 0.1 mol/L HCl and subsequently washed with hot distilled water to remove residual chemicals. The samples were then dried at 110°C in a hot air oven for final processing. Once dried, the activated carbon was pulverized into fine powder and sieved according to standard sieve sizes ($120\ \mu\text{m}$ and $170\ \mu\text{m}$), ensuring

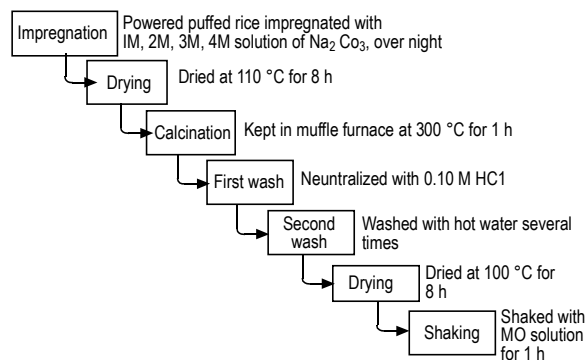


Fig. 2. Synthesis of Na_2CO_3 activated puffed rice biochar.

uniform particle size distribution for the adsorption experiments. Finally, the samples are pulverized into a fine powder and sieved according to standards, as depicted in Fig. 2.

Adsorption studies. Isotherm studies. Equilibrium studies. Langmuir and Freundlich adsorption isotherms are two models describing chemisorption, with Langmuir representing a monolayer adsorption process, while Freundlich describing the multilayer adsorption capability of the material.

Isotherm studies. An operational volume of 20 mL of synthetic effluent was used for batch adsorption investigations while changing the parameters. Included in the factors under investigation are the effects of phase contact time, MO concentration and temperature. After the equilibrium is reached, the results were noted. A UV visible spectrophotometer was used to measure the optical density at 462 nm after samples were taken out and filtered. This was used to calculate the MO concentration at equilibrium (C_e), the amount of MO adsorbed (q_e) and the percentage of adsorption. Adsorption percentage or dye removal was calculated using the following equation.

Nomenclature:

C_o = Initial concentration of methyl orange, MO; C_e = Methyl orange concentration at equilibrium, mg/L; q_e = Amount of methyl orange adsorbed on the adsorbent at equilibrium, mg/g; q_m = Maximum adsorption capacity, mg/g; K_d = Distribution coefficient for the adsorption, g/L; R_L = Favorability of adsorption; K_F = Freundlich constant, mg/g; K_L = Langmuir constant, L/mg; $1/n$ = Freundlich constant; T = Temperature K; M = Weight of biochar, g; E_a = Activation energy,

kJ/mol; MO = Methyl orange (sodium 4-[[4-(dimethylamino) phenyl] diazenyl] benzene-1-sulfonate, $C_{14}H_{14}N_3NaO_3S$); R = Universal gas constant, 8.314 J/mol/K; V = Volume, L; R^2 = Correlation coefficient; ΔS^\ddagger = Entropy of activation, J/K/mol; ΔH^\ddagger = Enthalpy of activation, kJ/mol; ΔG° = Gibbs free energy, kJ/mol; Suffix “e” = Equilibrium; Suffix “ini” = Initial

$$\% \text{ Dye adsorption} = \frac{C_0 - C_e}{C_0} \times 100 \quad (1)$$

$$q_e = \frac{C_0 - C_e}{M} \times V \quad (2)$$

where:

q_e , (mg/g) amount of MO adsorbed, C_0 (mg/L) and C_e (mg/L) are initial and equilibrium concentrations of MO in the liquid phase, respectively. Equilibrium, q_e (Anisuzzaman *et al.*, 2015; Thilagan *et al.*, 2013).

Langmuir isotherm. The amount of adsorption depends on the area of the adsorbent surface that is open. On the other hand, the extent of desorption depends on the amount of the adsorbent surface that is covered (Ayawei *et al.*, 2017; Anisuzzaman *et al.*, 2015; Deng *et al.*, 2009). After analyzing the adsorption isotherm data with the Langmuir isotherm model, the following linear form was obtained (Zhul-quarnain *et al.*, 2018; Hussaro *et al.*, 2014).

$$\frac{C_e}{q_e} = \frac{1}{q_m K_L} + \frac{C_e}{q_m} \quad (3)$$

$$R_L = \frac{1}{1 + R_L C_0} \quad (4)$$

Freundlich isotherm. This isotherm presents an equation that describes the surface heterogeneity and the exponential distribution of energy and active sites (Ayawei *et al.*, 2017). The Freundlich isotherm is represented in linear form as follows: where K_F represents the Freundlich adsorption constant, indicating the maximum adsorption capacity of MO (mg/g) and ‘n’ denotes the adsorption intensity constant (dimensionless).

$$\log q_e = \log K_L + \frac{1}{n} \log C_e \quad (5)$$

Adsorption thermodynamics. The thermodynamic parameters for methyl orange (MO) adsorption by activated carbon were determined using the following formulas,

as referenced by Thilagan *et al.* (2013) and Ozer *et al.* (2007). The values of the Gibbs free energy (ΔG°) at various temperatures were calculated. Additionally, the distribution coefficient K_d (g/L) for adsorption was determined and plotting $\log K_d$ against $1/T$ facilitated the determination of entropy change (ΔS^\ddagger) and enthalpy change (ΔH^\ddagger).

$$K_d = q_e / C_e \quad (6)$$

$$\Delta G^\circ = -2.303RT \log K_d \quad (7)$$

$$\log K_d = \frac{\Delta S^\ddagger}{2.303R} - \frac{\Delta H^\ddagger}{2.303RT} \quad (8)$$

The values of Gibbs free energy (ΔG°) at various temperatures were computed based on the experimental results.

Results and Discussion

Characterization of absorbent materials. FTIR Analysis. The FTIR spectra of Na_2CO_3 -activated puffed rice biochar are depicted in Fig. 3(a) and with the addition of MO in Fig. 3(b). In Fig. 3(a), the Fourier Transform Infrared Spectroscopy (FTIR) analysis of Na_2CO_3 activated puffed rice biochar revealed distinctive peaks at various wavenumbers indicative of its complex composition. Peaks detected at 3078.08/cm, 1380.08/cm, and 780.03/cm suggest the presence of aliphatic hydrocarbons (C-H medium bond (alkene), C-H medium bond (alkane) and C=C medium bond (alkene) (Doke *et al.*, 2013; Socrates, 2004). Peaks in the vicinity of 246.50/cm and 254.93/cm may suggest the presence of halogenated compounds or sulfur-containing functional groups. Furthermore, peaks like 457.03/cm indicate potential vibrations related to C-Cl stretching. These results indicate a mixed composition resulting from the activation process with Na_2CO_3 , comprising both inorganic and organic components. Further investigation and comparison with reference spectra are required to elucidate the functional groups present and their implications in biochar formation and potential applications.

The FTIR examination of Na_2CO_3 activated puffed rice biochar in Fig. 3(b) with the addition of MO dye revealed different peaks suggestive of molecular interactions and functional groups. Peaks observed at 3119.81/cm suggest the involvement of hydroxyl groups in hydrogen bonding (Baker, 1992) interactions with the dye molecules, while

those at 1381.21/cm indicate the persistence of aliphatic hydrocarbons on the biochar surface. Peaks in the regions of 461.18/cm and 236.54/cm suggest unaffected lattice vibrations of mineral components or metal-oxygen bonds. Peaks at 280.91/cm and 252.47/cm may indicate the presence of halogenated compounds or sulphur-containing functional groups, potentially interacting chemically with the dye molecules. These findings suggest that, while the addition of MO dye alters the FTIR spectrum of the biochar, the overall structural integrity and composition remains relatively unchanged, indicating potential efficacy in dye adsorption. Further investigations, including adsorption kinetics and isotherm studies, are warranted to comprehensively understand the mechanisms and effectiveness

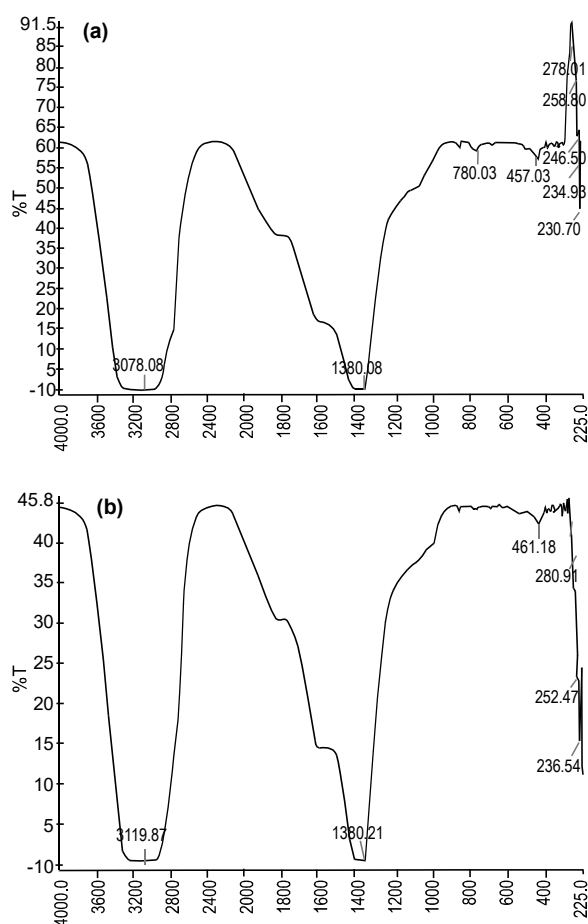


Fig. 3. FTIR spectrum of Na_2CO_3 activated puffed rice biochar; (a) and with MO (b) [Particle size = 170 μm ; Na_2CO_3] = 1.0 mol/L; [MO] = 29.599 mg/L; volume of MO = 20 mL; equilibration time = 60 min; temperature = 303 K].

of MO dye removal by Na_2CO_3 activated puffed rice biochar.

These investigations offer critical insights into the composition of biochar and its interactions with MO dye, essential for evaluating the biochar's adsorption efficiency. Post-treatment, alterations in the FTIR spectra suggest possible interactions between biochar's functional groups and MO dye molecules, such as chemical bonding or adsorption. It is expected that the spectra of Na_2CO_3 activated biochar treated with MO will exhibit changes in functional groups due to interactions with the dye. By comparing spectra, specific changes induced by the interaction can be identified, providing insights into the adsorption process and the potential utility of biochar in removing organic pollutants from wastewater.

SEM of Na_2CO_3 Activated puffed rice biochar analysis.

The SEM of Fig. 4(a), picture of Na_2CO_3 activated puffed rice biochar at a magnification of 2 μm reveals a porous structure with many small, homogeneous pores. These holes are critical to the material's adsorption performance because they provide a large surface area for contact with contaminants such as methyl orange. The figure shows that activation with Na_2CO_3 caused a large surface area containing micro and mesopores, necessary for dye removal in aquatic settings.

The SEM of Fig. 4(b), picture at 20 μm reveals the surface morphology of Na_2CO_3 activated biochar. At this magnification, the image shows more voids and a rough, uneven surface. The enhanced roughness and holes help to improve the biochar's adsorption capability by allowing more dye molecule interaction. This porous structure suggests that methyl orange diffuses efficiently into the coal matrix, which improves total adsorption.

This SEM image of Fig. 4(c), at 2 μm depicts the interaction of Na_2CO_3 activated biochar after adsorption of methyl orange (MO). When compared to Fig. 4(a), the surface appears less porous, showing that the dye molecules have filled many of the biochar's pores. As previously described, electrostatic interactions, hydrogen bonding, and π - π stacking are potential mechanisms for methyl orange adsorption. The reduced visibility of the pores suggests that the biochar's surface successfully trapped methyl orange molecules, demonstrate its strong adsorption potential.

The SEM of Fig. 4(d), depicts at 10 μm resolution shows the Na_2CO_3 activated biochar structure after interaction with MO. The previously visible pores

become less distinct, and the surface shape appears more compact. This shows that the dye was successfully adsorbed onto the biochar surface, filling the larger cavities and microscopic holes. The homogeneous coating indicates that the biochar efficiently collects and retains methyl orange molecules, which justifies its use in wastewater treatment applications.

These images show how Na_2CO_3 activated biochar's porous structure allows for active dye adsorption, making it an option material for environmental clean up.

XRD pattern analysis of Na_2CO_3 activated puffed rice biochar. The XRD pattern in Fig. 5(a) displays the diffraction peaks of Na_2CO_3 activated puffed rice biochar. The broad and less sharp peaks demonstrate the biochar's amorphous nature, indicating that it is predominantly composed of disordered carbon structures. This amorphous form is typical of biochar and plays

an important role in its adsorption abilities. The broad peak at 22° corresponds to the (2) plane of graphitic carbon but the lack of distinct crystalline peaks provides that the biochar has no appreciable crystallinity.

Figure 5(b) demonstrates the amorphous nature of the Na_2CO_3 activated puffed rice biochar, which is identical to 5(a). The large peaks found at 20° and 30° emphasize the chaotic carbonaceous structure. The absence of identifiable crystalline peaks indicates that the material retains a primarily amorphous phase, which increases its capability to absorb organic chemicals such as dyes. This structural profile is consistent with the porous character of biochar seen in SEM images, indicating active sites for adsorption.

Figure 5(c) shows the XRD pattern of Na_2CO_3 activated puffed rice biochar following adsorption with methyl orange. Peaks at 22° and 24° indicate minor structural

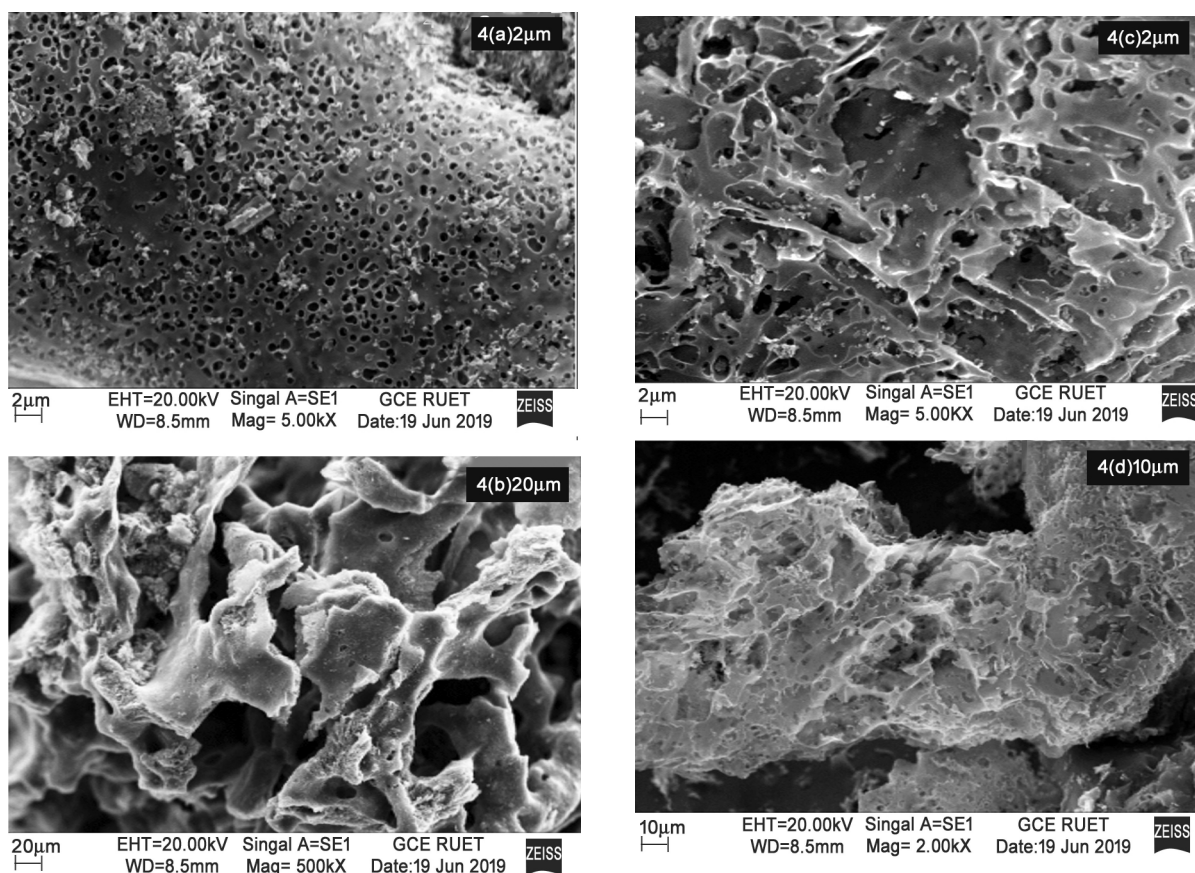


Fig. 4. SEM of Na_2CO_3 activated puffed rice biochar in (a) 2 μm and (b) 20 μm with MO (c) 2 μm and (d) 10 μm . Particle size = 170 μm ; $[\text{Na}_2\text{CO}_3]$ = 1.0 mol/L; $[\text{MO}]$ = 29.599 mg/L; volume of MO = 20 mL; equilibration time = 60 min; temperature = 30°C .

changes relative to raw biochar. The inclusion of methyl orange appears to marginally lessen the amorphous character, as evidenced by the sharper peaks. These slight alterations could be attributable to the interaction of dye molecules with biochar, leading to in some structural modification or surface adsorption-induced order.

The XRD pattern in Fig. 5(d) shows the structure of Na_2CO_3 activated puffed rice biochar following methyl orange adsorption. The traditional broad peaks remain, but minor increases in peak strength at 22° and 24° suggest that the adsorbed dye molecules have put some order into the amorphous matrix. It is due to π - π stacking interactions between the aromatic rings of methyl orange and the carbonaceous structure of the biochar, which can result in more ordered arrangements on the biochar surface. Shifts in peak positions and intensities at

different 2θ angles provide insights into structural changes in biochar.

The disappearing of the peak at 19° due to treatment, as opposed to the persistence of peaks at 12° and 24° , implies significant changes inside the material. This may highlight the impact of Na_2CO_3 activation on the biochar structure.

The XRD patterns illustrate the amorphous form of Na_2CO_3 activated puffed rice biochar, which is crucial for its adsorption capabilities. The modest modifications seen following methyl orange adsorption demonstrate the dye's successful interaction with the biochar, demonstrating that the biochar is appropriate for wastewater treatment applications. This characteristic is useful in applications that need the adsorption of contaminants like methyl orange. The presence of amorphous carbon, when combined with potential functional groups on the surface, boosts the material's adsorption capability, making these biochars acceptable options.

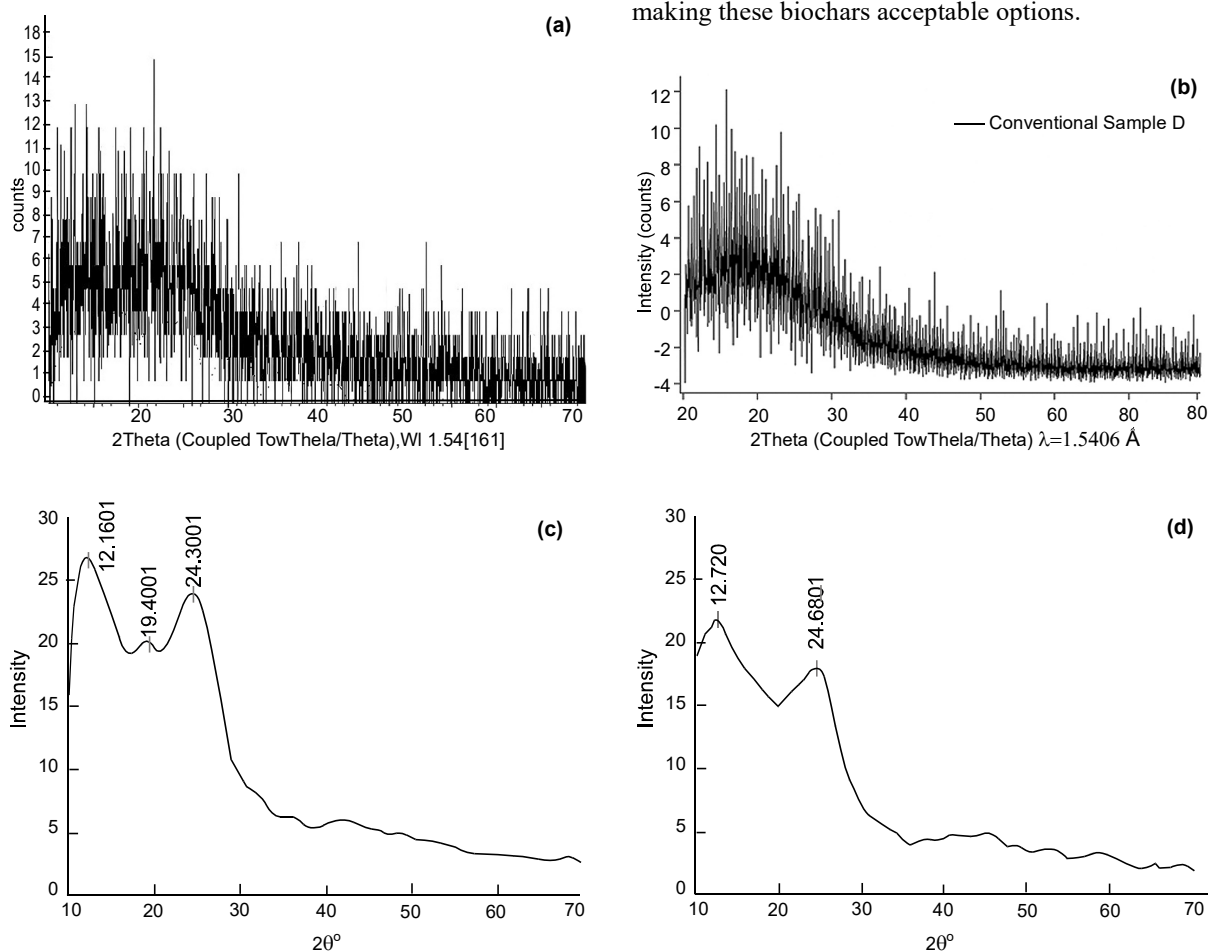


Fig. 5. XRD pattern of puffed rice biochar in (a) and (b) with MO in (c) and (d); particle size = $170 \mu\text{m}$; $[\text{MO}] = 29.599 \text{ mg/L}$; volume of MO = 20 mL; equilibration time = 60 min; temperature = 30°C .

Equilibrium studies. Impact of shaking time on the MO adsorption by puffed rice biochar.

The effect of shaking time on MO adsorption by biochar obtained from puffed rice is depicted in Fig. 6(a). The figure depicts the impact of shaking time on the adsorption of MO by Na_2CO_3 activated puffed rice biochar for different biochar sample weights (1.5 g, 1.0 g and 0.5 g). The x-axis (Time, min) represents the shaking time, while the y-axis ($[\text{MO}] C_e$ mg/L) shows the equilibrium concentration of MO (C_e) using equations 1 and 2. As shaking time increases from 4 min to 64 min, the equilibrium concentration of MO decreases, indicating that the adsorption efficiency improves with increased contact time between the biochar and the MO solution.

The 1.5 g sample consistently exhibits the lowest C_e values over time, indicating the highest adsorption efficiency, followed by the 1.0 g and 0.5 g samples. This trend suggests that a greater amount of biochar results in more available active sites for MO adsorption, thus reducing the concentration of MO in the solution more effectively. Additionally, the decrease in C_e values over time indicates that adsorption approaches equilibrium as more dye molecules are captured on the biochar surface.

The data suggest that the adsorption process is time dependent, with longer contact times allowing for greater interaction between MO and the biochar's active sites. This behavior aligns with typical adsorption kinetics, where the rate of adsorption is initially fast due to the

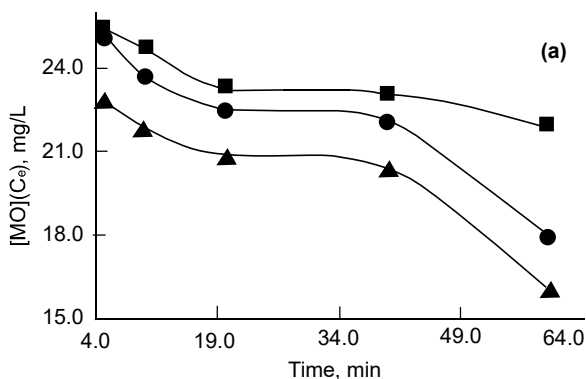


Fig. 6(a). The Impact of shaking time on the adsorption of MO by Puffed rice biochar; particle size = 120 μm ; temperature = 303 K; $[\text{MO}] = 29.599$ mg/L; volume of MO = 20 mL. (\blacktriangle) 1.5 g (\bullet) 1.0 g (\blacksquare) 0.5 g.

availability of a large number of active sites, followed by a slower rate as the surface approaches saturation (Ayawei *et al.*, 2017). The trend supports the conclusion that both the amount of biochar and the shaking time are critical factors for optimizing the adsorption process.

Langmuir isotherm: Shaking time study. Equation (3) represents the Langmuir isotherm model and adsorption isotherm experimental data for the biochar particle size of 120 μm is displayed in 6(b) as C_e/q_e vs C_e in order to generate this model. The slope and its intercept, R^2 values, which were also shown in Fig. 6(b) and calculated the values of q_m (mg/g) and K_L (L/mg). The obtained q_m values for 120 μm particle size were 0.04, 0.04 and 0.04 for 0.5 g, 1.0 g and 1.5 g, respectively. Conversely, K_L values for 0.5 g, 1.0 g and 1.5 g are calculated to be -0.05, -0.06 and -0.08, respectively. The R_L value is computed using the estimated values of q_m and K_L .

The Langmuir isotherm indicates a high level of efficiency in the process, implying that the surface area has been effectively utilized. The favourability of the adsorption process can be determined by calculating the separation factor (R_L) using eq. (4). The R_L value indicates the nature of the isotherm, suggesting it is irreversible ($R_L = 0$), favourable ($0 < R_L < 1$), linear ($R_L = 1$) and unfavourable ($R_L > 1$) (Kareem, 2016; Mulugeta and Lelisa, 2014). However, R_L values for 0.5g, 1.0 g

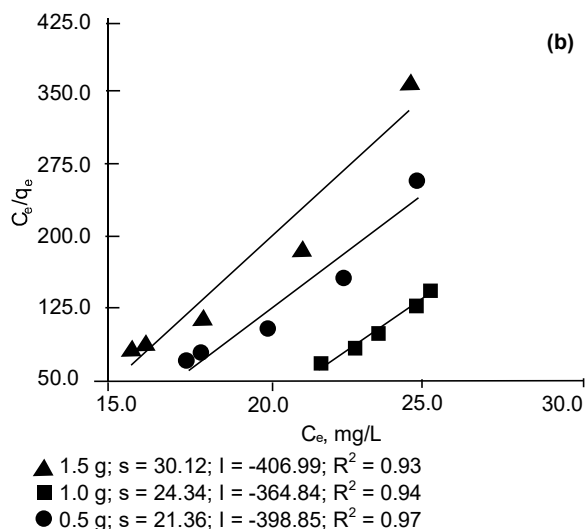


Fig. 6(b). The influence of shaking time on MO adsorption by puffed rice biochar (Langmuir plot); particle size = 120 μm ; temperature = 303 K; $[\text{MO}] = 29.599$ mg/L; volume of MO = 20 mL.

and 1.5 g at 120 μm particle size are -1.81, -1.16 and -0.75, respectively. The determined relative linearities (R_L) for the 120 μm puffed rice biochar particle size are smaller than zero in all cases, indicating the favourability of the MO adsorption process by the prepared puffed rice biochar.

Freundlich isotherm. Shaking time study. Equation (5) represents the Freundlich isotherm model and Fig. 6(c) shows a plot of $\log(C_e, \text{mg/L})$ vs $\log(q_e, \text{mg/g})$. K_F and $1/n$ values were estimated *via* intercepts and slopes of the plots, respectively and R^2 values were recorded. The adsorption coefficient or K_F (L/g), represents the quantity of dye adsorbed onto activated carbon adsorbent at the specified equilibrium concentration. The experimental results indicated that the K_F values for 120 μm particles were 40.243, 39.924 and 2.359 for 0.5 g, 1.0 g and 1.5 g correspondingly.

Measure of surface heterogeneity $1/n$ or adsorption intensity that ranges from 0 to 1, with a value approaching zero and becoming more heterogeneous. A number below one (1.0) represents a normal Freundlich isotherm but $1/n$ above one (1.0) suggests collective adsorption (Ayawei *et al.*, 2017; Doke *et al.*, 2013). In each cases, Fig. 6(c) for 120 μm particle size gives straight line with slope values -1.91, -2.75 and -4.11 for 1.5 g, 1 g and 0.5 g respectively. Thus, it is revealed that the

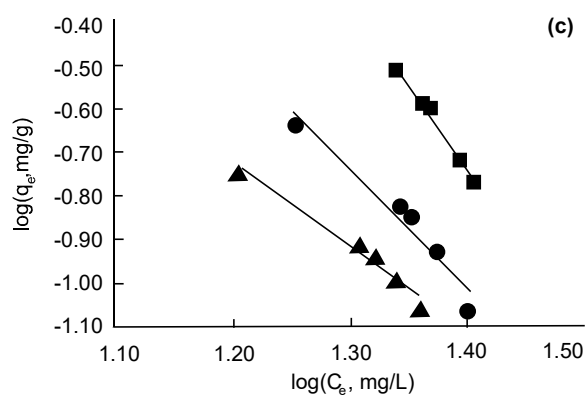


Fig. 6(c). The impact of shaking time on MO adsorption (Freundlich Plot); particle size = 120 μm ; temperature = 303 K; $[\text{MO}] = 29.599 \text{ mg/L}$; volume of MO = 20 mL; (\blacktriangle) 1.5 g; $s = -1.91$; $I = 1.57$; $R^2 = 0.98$ (\bullet); 1.0 g; $s = -2.75$; $I = 2.84$; $R^2 = 0.95$ (\blacksquare) 0.5 g; $s = -4.11$; $I = 5.01$; $R^2 = 0.99$.

adsorption of MO by puffed rice biochar do not follow the Freundlich isotherm for the studied system.

Particle size's impact on MO adsorption by puffed rice biochar. The Fig. 7(a) illustrates the impact of biochar particle size on the adsorption of methyl orange (MO) by Na_2CO_3 activated puffed rice biochar for different sample weights (1.5 g, 1.0 g and 0.5 g). The x-axis represents the particle size in micrometers (μm), while the y-axis shows the equilibrium concentration of MO (C_e) in mg/L, calculated using equation (1) and (2). The data indicate that as the particle size increases from 70 μm to 170 μm , the equilibrium concentration of MO decreases for all biochar sample weights. This suggests that smaller particle sizes lead to more efficient adsorption, as indicated by the lower C_e values, which reflect higher adsorption capacity.

Smaller particles generally have a larger surface area-to-volume ratio, offering more active sites for MO adsorption (Kareem *et al.*, 2016). Among the different sample weights, the 1.5 g sample consistently exhibits the lowest C_e values, indicating the highest adsorption efficiency, followed by the 1.0 g and 0.5 g samples. This trend highlights that both the particle size and the amount of biochar used significantly influence the adsorption capacity, with smaller particle sizes and larger biochar quantities leading to improved MO removal. The results align with prior studies showing that smaller biochar particles tend to offer better

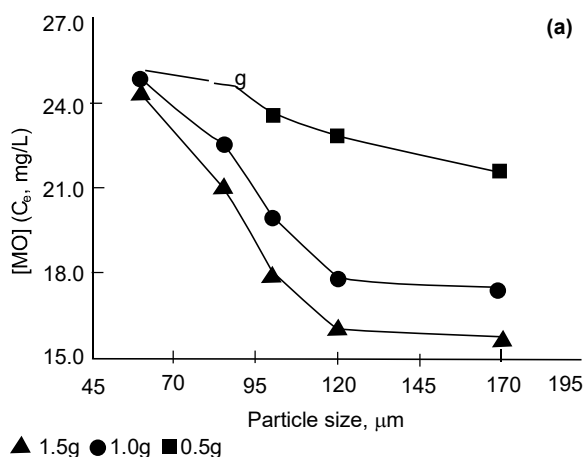


Fig. 7(a). Particle size's impact on MO adsorption by puffed rice biochar; temperature = 303 K; $[\text{MO}] = 29.599 \text{ mg/L}$; volume of MO = 20 mL; equilibration time = 60 min.

adsorption performance due to the increased availability of surface area and active sites (Ayawei *et al.*, 2017).

Langmuir isotherms. Particle size study. Figure 7(b) presents a Langmuir plot illustrating the effect of particle size on the adsorption of methyl orange (MO) by puffed rice biochar. The plot demonstrates a strong linear relationship between the equilibrium concentration of MO (C_e) and C_e/q_e for biochar weights of 1.5 g, 1.0 g and 0.5 g, indicating that the adsorption process adheres to the Langmuir isotherm. With the larger biochar particles (1.5 g) exhibit higher adsorption capacity due to increased surface area and more available adsorption sites, as reflected by steeper slopes and lower C_e/q_e values. The highest adsorption efficiency is observed for the 1.5 g biochar, followed by 1.0 g and 0.5 g samples. The high R^2 values (0.93 to 0.97) confirm a strong fit to the Langmuir model which suggests monolayer adsorption on a homogenous surface.

The Langmuir isotherm model, as described by equation (3), assumes that adsorption occurs on a uniform surface with energetically identical adsorption sites, which is reflected in the linearity of the plot. The values of the maximum adsorption capacity (q_m) were calculated as

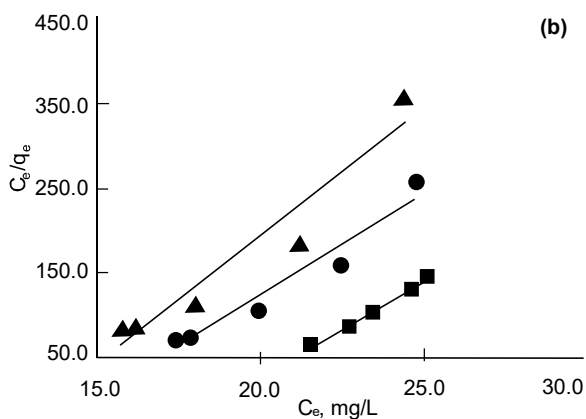
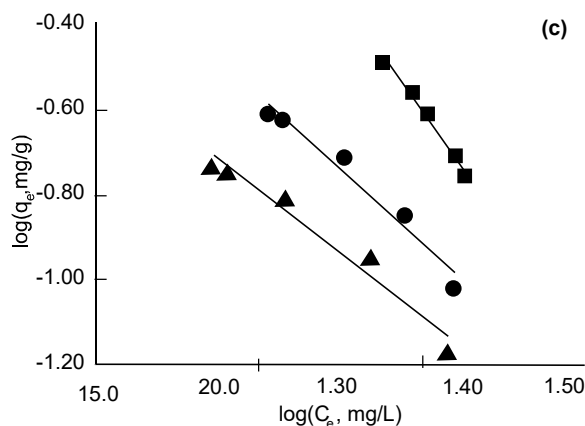


Fig. 7(b). Effect of particle size on the adsorption of MO by puffed rice biochar (Langmuir plot); temperature = 303 K; [MO] = 29.599 mg/L; volume of MO = 20 mL; equilibration time = 60 min; temperature = 303 K; [MO] = 29.599 mg/L; volume of MO = 20 mL; equilibration time = 60 min (▲) 1.5 g; $s = 30.12$; $I = -406.99$; $R^2 = 0.93$ (●) 1.0 g; $s = 24.34$; $I = -364.84$; $R^2 = 0.94$ (■) 0.5 g; $s = 21.36$; $I = -398.85$, $R^2 = 0.97$.

0.09, 0.06 and 0.05 mg/g for the 0.5 g, 1.0 g and 1.5 g biochar samples, respectively, while the Langmuir constant (K_L) values were -0.87, -1.64 and -3.21 L/mg for the same weights. The separation factor (R_L), which indicates the favourability of adsorption, was calculated as -0.20, -0.09 and -0.05 for 0.5 g, 1.0 g and 1.5 g, respectively. These R_L values suggest that the adsorption process is more favourable at higher MO concentrations and less favourable at lower concentrations.

In conclusion, the Langmuir isotherm effectively models the adsorption process, as it assumes monolayer adsorption on a uniform surface with no interactions between adsorbed molecules. This model provided a better fit to the experimental data compared to the Freundlich isotherm, affirming its suitability for describing the adsorption of MO onto puffed rice biochar in this study.

Freundlich isotherms. Particle size study. The Freundlich isotherm portrays surface heterogeneity and the exponential distribution of active sites and their energies, delineating adsorption on a heterogeneous surface with uniform energy where interactions between adsorbed molecules are not confined to monolayer formation (Haitham *et al.*, 2014). A linear relationship is depicted in Fig. 7(c), plotting $\log(C_e, \text{mg/L})$ against $\log(q_e, \text{mg/g})$, with the Freundlich isotherm model



▲ 1.5 g; $s = -2.19$, $I = 1.90$, $R^2 = 0.97$
● 1.0 g; $s = -2.56$, $I = 2.59$, $R^2 = 0.97$
■ 0.5 g; $s = -3.92$, $I = 4.74$, $R^2 = 0.98$

Fig. 7(c). Effect of particle size on the adsorption of MO by puffed rice biochar (Freundlich plot); temperature = 303 K; [MO] = 29.599 mg/L; volume of MO = 20 mL; equilibration time = 60 min.

represented in Eq. (6). The values of K_F (L/g) and $1/n$ were derived from the intercept. K_F signifies the amount of dye adsorbed onto activated carbon adsorbent per unit equilibrium concentration, calculated as 0.31, 0.12 and -0.07 for 0.5 g, 1.0 g and 1.5 g of puffed rice biochar, respectively. The graph exhibits a negative slope for each experimental set, resulting in $1/n$ values of -0.21, -0.38 and -0.66 for 1.5 g, 1 g and 0.5 g of puffed rice biochar, respectively. The 0.5 g biochar sample shows the highest adsorption capacity, attributed to its greater surface area and increased availability of active sites for MO adsorption. The high R^2 values (0.97 to 0.98) across all particle sizes confirm the strong linearity of the relationship, reinforcing that smaller biochar particles are more effective at adsorbing MO. The $1/n$ parameter serves as a measure of surface heterogeneity or adsorption intensity, ranging from 0 to 1, with values closer to zero indicating greater heterogeneity. A normal Freundlich isotherm is indicated by a $1/n$ value less than one, while collective adsorption is indicated by a value greater than one (Ayawei *et al.*, 2017; Kareem, 2016). The experimental results suggest that the system is not suitable for the Freundlich isotherm model.

The impact of Na_2CO_3 concentration on puffed rice biochar's activation for MO adsorption. The graph in Fig. 8(a) illustrates the impact of varying Na_2CO_3 concentrations on the adsorption of MO by puffed rice

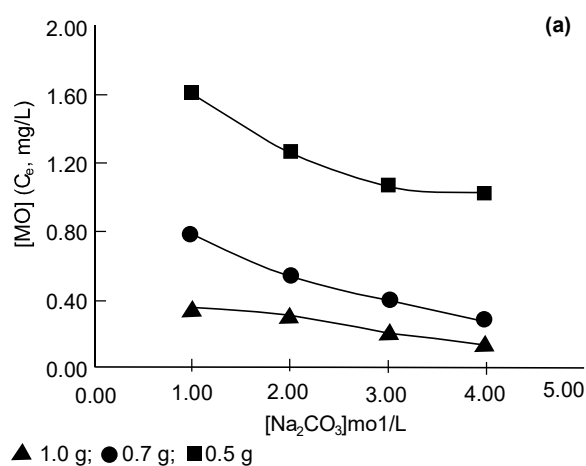


Fig. 8(a). The impact of different concentrations of Na_2CO_3 activated puffed rice biochar on MO adsorption; particle size = 170 μm ; temperature = 303 K; $[\text{MO}] = 29.599$ mg/L; volume of MO = 20 mL; time = 60 min.

biochar, activated at different weights (0.5 g, 0.7 g and 1.0 g). The x-axis represents Na_2CO_3 concentrations (mol/L), while the y-axis shows the equilibrium concentration of MO (C_e , mg/L). The general trend reveals that as the Na_2CO_3 concentration increases, the equilibrium concentration of MO decreases for all biochar weights, indicating improved adsorption capacity with higher Na_2CO_3 concentrations.

The 0.5 g biochar sample shows the highest C_e values, meaning it has the lowest adsorption efficiency. In contrast, the 1.0 g sample, indicated by the triangular markers, exhibits the lowest C_e values across all Na_2CO_3 concentrations, suggesting it has the highest adsorption capacity. As the Na_2CO_3 concentration increases from 1.0 to 4.0 mol/L, the adsorption of MO consistently improves across all biochar weights, with steeper reductions in C_e for larger biochar weights. This suggests that increasing both the Na_2CO_3 concentration and biochar weight significantly enhances the biochar's ability to adsorb MO, likely due to increased surface area and more active adsorption sites. This suggests that the optimal conditions for maximum adsorption of MO involve higher Na_2CO_3 concentrations around (4.0 mol/L) and using more biochar (1.0 g), as these factors provide more active sites for MO adsorption. The data obtained from the adsorption of MO onto activated carbon were subjected to analysis using the Langmuir and Freundlich isotherms.

Langmuir isotherm for Na_2CO_3 activation of puffed rice biochar. The Langmuir plot for the adsorption of methyl orange (MO) onto Na_2CO_3 activated puffed rice biochar shows a clear linear relationship between C_e/q_e and C_e at various biochar concentrations. This linearity aligns with the Langmuir isotherm model, as described by equation (3) and is further illustrated in Fig. 8(b) which plots C_e/q_e against C_e (mg/L). This confirms the model's assumption of monolayer adsorption onto a homogenous surface with uniform adsorption sites. A strong linear correlation was observed across all experimental conditions, with the values of q_m (mg/g) and K_L (L/mg) derived from the slope and intercept of the linear plot.

As the concentration of Na_2CO_3 activated biochar increases from (0.5 g to 1.0 g), the slope of the plot becomes steeper, indicating that higher Na_2CO_3 concentrations enhance adsorption capacity by providing more active sites for MO adsorption. The increased slopes at higher Na_2CO_3 concentrations demonstrate

the biochar's improved efficiency in adsorbing MO, highlighting the importance of Na_2CO_3 activation in optimizing adsorption performance. The R^2 value of 1 for each experimental condition confirms a perfect fit for the Langmuir model, indicating that the adsorption process closely follows this isotherm. The obtained q_m values were 1.08, 0.81 and 0.58 mg/g for 0.5 g, 0.7 g and 1.0 g of activated puffed rice biochar, respectively. The corresponding K_L values were -18.59, -123.00 and -573.33, indicating increasing adsorption efficiency with greater biochar activation.

The Langmuir isotherm suggests efficient surface utilization, as the process is shown to be reasonably effective. The favorability of the adsorption process was further assessed using the separation factor (R_L), calculated with equation (4). R_L values classify isotherms as unfavourable ($R_L > 1$), linear ($R_L = 1$), favourable ($0 < R_L < 1$) or irreversible ($R_L = 0$). The R_L values for 0.5 g, 0.7 g and 1.0 g of activated puffed rice biochar were -0.002, -0.0003 and -0.00006, respectively. These negative R_L values confirm the favourability of the adsorption process for this system, affirming that the adsorption of MO onto Na_2CO_3 activated puffed rice biochar follows the Langmuir isotherm model efficiently.

Freundlich isotherm for Na_2CO_3 activation of puffed rice biochar. The isotherm provides an expression that

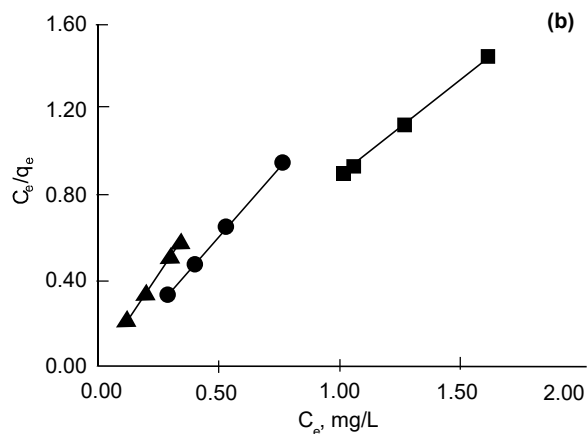


Fig. 8(b). Impact of Na_2CO_3 concentration on MO adsorption (Langmuir Plot); particle size = 170 μm ; temperature = 303 K; $[\text{MO}] = 29.599 \text{ mg/L}$; volume of MO = 20 mL; time = 60 min (\blacktriangle) 1.0 g, $s = -0.007$; $I = -0.024$; $R^2 = 0.99$ (\bullet) 0.7 g; $s = -0.0017$; $I = -0.09$; $R^2 = 0.97$ (\blacksquare) 0.5 g; $s = -0.05$; $I = 0.06$; $R^2 = 0.99$.

delineates the surface heterogeneity and exponential distribution of active sites and their energies. In Fig. 8(c) the plot of $\log(C_e, \text{mg/L})$ vs $\log(q_e, \text{mg/g})$ illustrates the Freundlich adsorption isotherm. The Freundlich isotherm model is represented by eq. (5), where the values of $K_F(\text{L/g})$ and $1/n$ are determined from intercepts and slopes in Fig. 8(c), respectively.

The value of K_F serves as the adsorption coefficient, indicating the quantity of dye adsorbed onto the activated carbon adsorbent for a unit equilibrium concentration. The estimated K_F values are 1.15, 0.81 and 0.56 for 0.5 g, 0.7 g and 1.0 g of activated puffed rice biochar, respectively.

The values of $1/n$, lying between 0 and 1, represent the degree of adsorption intensity or surface heterogeneity, with a tendency to become more heterogeneous as the value approaches zero. A value for $1/n$ below one indicates a typical Freundlich isotherm, while a value above one suggests collective adsorption (Ayawei *et al.*, 2017; Kareem, 2016).

In Fig. 8(c) each set of experimental parameters under investigation yields a straight line with a negative slope. The calculated slope values are -0.007, -0.017 and -0.05 for 1.0 g, 0.7 g and 0.5 g of activated puffed rice

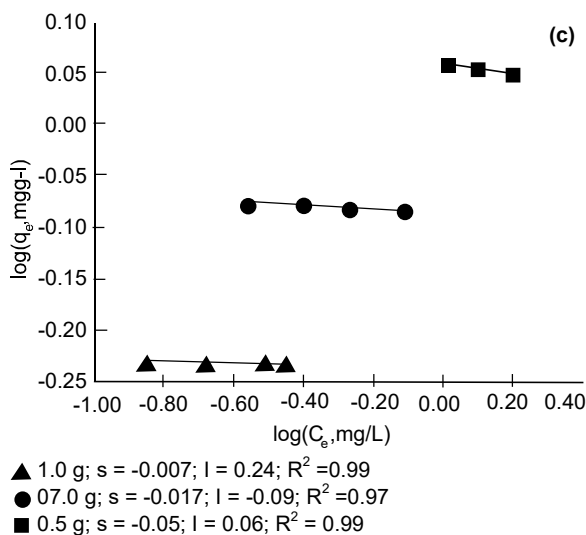


Fig. 8(c). The influence of Na_2CO_3 concentration in activating puffed rice biochar on MO adsorption (Freundlich plot); [particle size = 170 μm ; temperature = 303 K; $[\text{MO}] = 29.599 \text{ mg/L}$; volume of MO = 20 mL; time = 60 min].

biochar, respectively. Thus, the system under investigation does not adhere to the Freundlich adsorption isotherm.

Impact of temperature's on Na_2CO_3 activation for MO adsorption by puffed rice activated carbon. The graph in Fig. 9(a) shows the effect of temperature on the adsorption of methyl orange (MO) by Na_2CO_3 activated puffed rice biochar, comparing two concentrations of Na_2CO_3 (1.0 mol/L and 2.0 mol/L). The graph illustrates the effect of temperature on the adsorption of methyl orange (MO) by Na_2CO_3 activated puffed rice biochar, comparing two different Na_2CO_3 concentrations. As temperature increases, the adsorption capacity (q_e) rises for both concentrations, indicating that the adsorption process is endothermic. The biochar activated with 2.0 mol/L Na_2CO_3 consistently exhibits a higher adsorption capacity than the biochar activated with 1.0 mol/L across all temperatures, suggesting that a higher Na_2CO_3 concentration enhances the biochar's adsorption efficiency. The experiment used an aqueous solution of MO (23.28 mg/L), with 20 mL of the solution equilibrated with 0.5 g of biochar at varying temperatures (20 °C to 40 °C).

The graph also demonstrates the relationship between the equilibrium concentration of MO (C_e) and tempera-

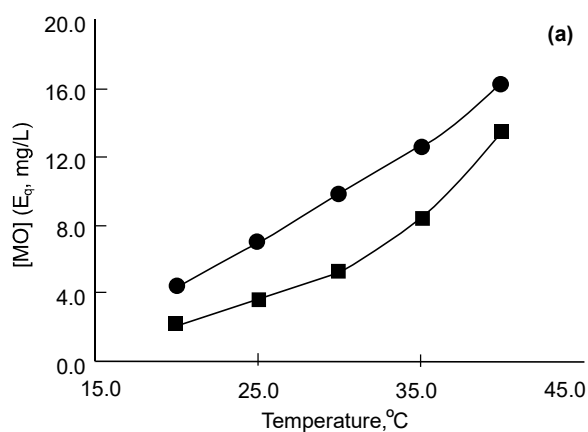


Fig. 9(a). Impact of temperature on Na_2CO_3 activation for the adsorption of MO by puffed rice activated carbon (●) [Na_2CO_3] = 2.0 mol/L; (■) [Na_2CO_3] = 1.0 mol/L; particle size = 170 μm ; weight of activated puffed rice bio char = 0.5 g; [MO] concentration = 23.28 mg/L; volume of MO = 20 mL; time = 60 min.

ture. As temperature increases, adsorption capacity improves, reflecting stronger interactions between the dye and biochar. This effect is more pronounced for the higher Na_2CO_3 concentration, which further highlights its role in enhancing adsorption. However, while the 2.0 mol/L Na_2CO_3 concentrations shows a consistent increase in adsorption capacity with temperature, the 1.0 mol/L concentration reveals a decrease in both C_e and q_e as temperature rises, leading to lower adsorption efficiency. Based on the graph and the graphical trend, higher temperatures improve the adsorption capacity for both Na_2CO_3 concentrations, with the best performance observed around 40 °C approximately (313 K). The inconsistent trends observed in C_e/q_e and K_d with temperature, as calculated using equations 2 and 6, indicate that temperature has a significant impact on the thermodynamic parameters of the adsorption process for both Na_2CO_3 concentrations. This suggests that temperature not only influences the adsorption capacity but also affects the equilibrium and distribution of MO between the biochar and solution, leading to variations in adsorption efficiency.

In conclusion, while increasing temperatures initially improve adsorption efficiency by enhancing MO molecule diffusion into the biochar's pores, higher temperatures may also negatively impact adsorption by altering the surface properties of the biochar, particularly for the 1.0 mol/L Na_2CO_3 concentration. The results emphasize that both Na_2CO_3 concentration and temperature play critical roles in optimizing the biochar's adsorption performance.

Langmuir isotherm. Temperature impacts on the adsorption of MO by Na_2CO_3 activated biochar. This model has found widespread application in various monolayer adsorption processes. The data from adsorption isotherms are commonly analyzed using the linearized form of the Langmuir model (Baker *et al.*, 1992).

The Langmuir isotherm model is described by eq. (3) and illustrated as C_e/q_e vs. (C_e , mg/L) in Fig. 9(b). The slope and intercept yielded q_m (mg/g) values of 0.19 and 0.36, as well as K_L (L/mg) values of -0.19 and -0.46, for Na_2CO_3 concentrations of 1.0 and 2.0 mol/L, respectively. The linearity of the plots confirms that the adsorption of MO onto Na_2CO_3 activated puffed rice biochar follows the Langmuir isotherm, which suggests monolayer adsorption on a homogenous surface. The arrows indicate shifts in experimental conditions, which

result in different adsorption capacities and equilibrium concentrations. This figure demonstrates that under varying conditions, the biochar effectively adsorbs MO, with the Langmuir model providing a reliable representation of the adsorption behaviour. The plot shows two distinct linear trends, each corresponding to different sets of experimental conditions or adsorption parameters, such as variations in particle size, Na_2CO_3 concentration. Langmuir isotherm indicates that the process is reasonably efficient; meaning total utilization of surface area has been sufficiently done. The favorability of the adsorption process is calculated from the separation factor (R_L) by using equation (4). The R_L value categorizes the isotherm as:

Unfavourable when $R_L > 1$; linear when $R_L = 1$; Favourable when $0 < R_L < 1$ and Irreversible when $R_L = 0$ (Kareem, 2016; Mulugeta and Lelisa, 2014). The R_L values calculated for Na_2CO_3 concentrations of 1.0 mol/L and 2.0 mol/L were -0.29 and -0.10, respectively. The stated experimental results reveal the favourability of adsorption process. However, the positive slope of the Langmuir plot shows that the system under investigation follows the Langmuir adsorption isotherm model.

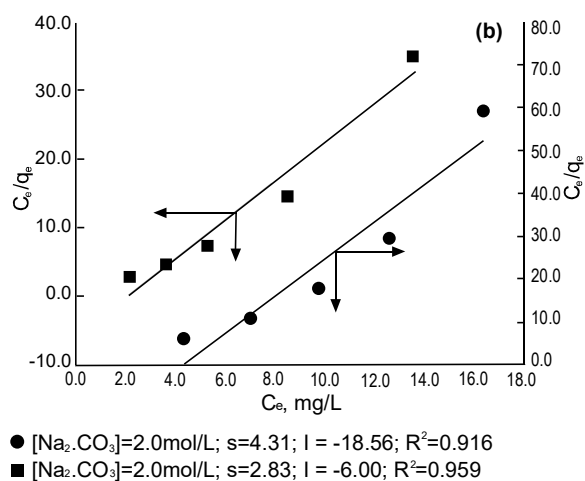


Fig. 9(b). Effect of temperature on Na_2CO_3 activation for the adsorption of MO by activated carbon from puffed rice (Langmuir plot); [particle size = 170 μm ; weight of activated puffed rice biochar = 0.5 g; [MO] concentration = 23.28 mg/L; volume of MO = 20 mL, time = 60 min].

Freundlich isotherm. Temperature impacts on the adsorption of MO by Na_2CO_3 activated biochar. The Freundlich isotherm model represented in equation (5) and plotted as $\log(C_e, \text{mg/L})$ vs $\log(q_e, \text{mg/g})$, in Fig. 9(c). This type of plot is characteristic of the Freundlich isotherm, which describes adsorption on a heterogeneous surface and suggests multilayer adsorption. The two distinct linear trends likely represent adsorption data for different experimental conditions, such as varying Na_2CO_3 concentrations, particle sizes or adsorbent amounts.

The values of K_F (L/g) and $1/n$ were obtained from the slope and intercepts of figure respectively. K_F denotes the adsorption coefficient, signifying the quantity of dye adsorbed per unit equilibrium concentration onto the activated carbon adsorbent. For Na_2CO_3 concentrations of 1.0 and 2.0 mol/L, the corresponding K_F (L/g) values were determined as 4.07 and 10.0, respectively. The parameter $1/n$, varying between 0 and 1, delineates the degree of adsorption intensity or surface heterogeneity, with lower values indicating higher heterogeneity. And the values below one indicate a typical Freundlich isotherm, while values above one suggest cooperative adsorption (Kareem *et al.*, 2016; Ji *et al.*, 2007). The two distinct straight lines have negative slopes, calculated as -0.41 and -0.72 for Na_2CO_3 concentrations of 1.0 mol/L and 2.0 mol/L, respectively and the regression

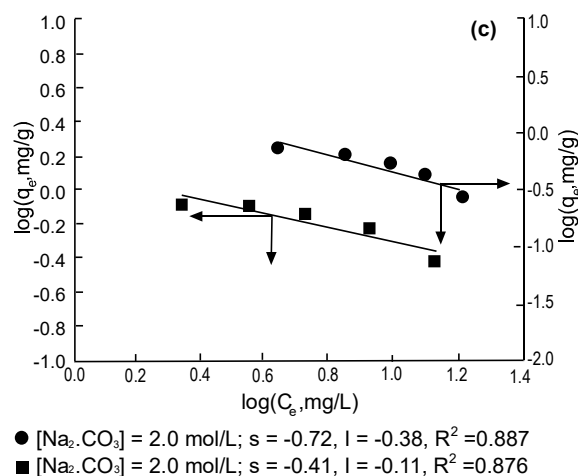


Fig. 9(c). Temperature's impact on Na_2CO_3 activated puffed rice for MO adsorption (Freundlich isotherm); [particle size = 170 μm ; weight of biochar = 0.5 g; [MO] = 23.28 mg/L; volume of MO = 20 mL, time = 60 min].

coefficients (R^2 values) are not close to 1. The negative slope indicates a divergence from the Freundlich adsorption isotherm, implying that the system under investigation does not conform to the Freundlich model.

Chemical reaction of MO and Na_2CO_3 . The interaction between methyl orange (MO) and sodium carbonate typically involves the transfer of a proton from MO to the carbonate ion (CO_3^{2-}) within sodium carbonate. This chemical process can be illustrated as:



During this reaction, the protonated form of methyl orange (MOH^+) reacts with the carbonate ion, resulting in the formation of a negatively charged methyl orange ion (MO^-), along with carbon dioxide (CO_2) and water (H_2O). This proton transfer changes the chemical structure of methyl orange, enhancing its ability to adhere to the surface of the adsorbent material. Essentially, the acidic proton of MO gets neutralized by the basic carbonate ion (CO_3^{2-}) in sodium carbonate, constituting a neutralization reaction.

Thermodynamics for the Na_2CO_3 activated puffed rice biochar. The Gibbs free energy values (ΔG°) for different temperatures are determined using equation (7), based on the experimental data provided in Table 1. The enthalpy change (ΔH^\pm) and entropy change (ΔS^\pm) are then estimated from the slope and intercept of the plot of $\log K_d$ vs $(1/T) \times 10^3$, where K_d is the dissociation constant. The plot is not displayed in this section. However, the thermodynamic parameters, calculated using equation (6), (7) and (8) which are presented in Table 1 for reference.

Table 1 shows the thermodynamic parameters for adsorbing methyl orange (MO) onto Na_2CO_3 activated charcoal at varied Na_2CO_3 concentrations and temperatures. The Gibbs free energy (ΔG°) values for 1.0 mol/L and 2.0 mol/L Na_2CO_3 concentrations show that adsorption becomes less spontaneous as temperature increases from 293 K to 313 K, with ΔG° values shifting from lower to higher positive values. This tendency indicates that greater temperatures reduce the spontaneity of the adsorption process. MO adsorption on biochar is exothermic, as demonstrated by the negative enthalpy change (ΔH^\pm) at both concentrations. The ΔH^\pm value for 1.0 mol/L Na_2CO_3 is -98.03 kJ/mol, while for 2.0 mol/L, it is -87.50 kJ/mol, indicating a minor decrease in the exothermic nature with increasing Na_2CO_3 concentrations. Additionally, both concentrations have a negative entropy change (ΔS^\pm), indicating a decrease in disorder at the solid-liquid interface after adsorption. The entropy change is more negative at 1.0 mol/L (-341.59 J/mol K) than 2.0 mol/L (-312.67 J/mol K), indicating a higher loss of randomness at the surface with the lower Na_2CO_3 concentration. However, the data indicates that the adsorption process is exothermic, getting less spontaneous with the temperature raises, results in decreased entropy, with both thermodynamic properties being slightly concentration-dependent.

Future research directions. Future research on Na_2CO_3 -activated puffed rice biochar should explore several areas to enhance its effectiveness and broaden its applications. Investigating the effect of pH on adsorption could optimize conditions for treating different types of wastewater. Additionally, studying the regeneration

Table 1. Evaluation of thermodynamic parameters for the adsorption of methyl orange (MO)

$[\text{Na}_2\text{CO}_3]$, mol/L	Temperature, K	ΔG° (J/mol)	ΔH^\pm (kJ/mol)	ΔS^\pm (kJ/mol K)
1.0	293	5291.545	-98.03	-341.59
	298	3731.245		
	303	5016.144		
	308	6819.07		
	313	9239.063		
2.0	293	4250.543	-87.50	-312.67
	298	5862.729		
	303	7292.074		
	308	8657.223		
	313	10607.29		

Particle size = 170 μm ; $[\text{MO}] = 23.28$ mg/L; Volume of MO = 20 mL; Time = 60 min; Weight of Na_2CO_3 activated bio char = 0.50 g]

and reusability of the biochar over multiple cycles is crucial for assessing its sustainability and cost efficiency in long-term use. Expanding the application to other pollutants, such as heavy metals and pharmaceuticals, could further demonstrate its versatility in environmental remediation. Research on continuous systems, such as fixed bed reactors, would provide more practical insights into its performance under real-world conditions. Surface modification techniques could also be explored to improve the biochar's adsorption capacity and selectivity. Finally, conducting environmental and economic feasibility studies would help determine the scalability and cost effectiveness of using Na_2CO_3 activated biochar in industrial wastewater treatment. Together, these research directions could significantly enhance the potential of this biochar for broader environmental applications.

Molecular-level mechanism of methyl orange adsorption from wastewater onto Na_2CO_3 activated puffed rice biochar. Figure 10 illustrates the molecular mechanism by which Na_2CO_3 -activated puffed rice biochar adsorbs methyl orange dye. This process is driven by three key interactions: electrostatic attraction, hydrogen bonding and π - π interactions. The negatively charged sulfonic groups in methyl orange are attracted to positively charged sites on the biochar surface, forming electrostatic bonds. Simultaneously, hydrogen bonds form between the biochar's hydroxyl groups and the azo groups in the dye. Additionally, π - π stacking

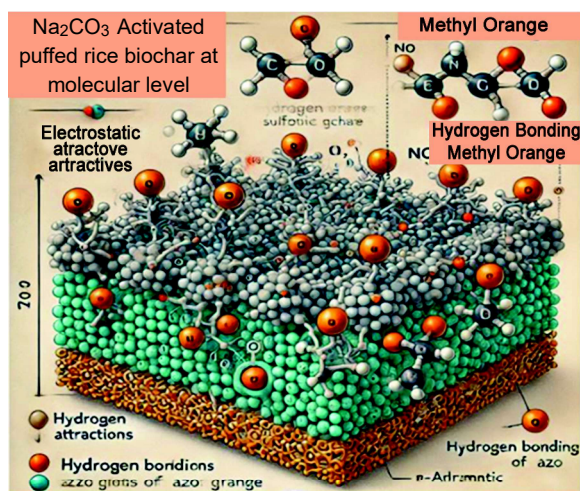


Fig 10. Interaction between methyl orange dye and Na_2CO_3 activated puffed rice biochar (ChatGpt AI Generated).

occurs between the aromatic rings of methyl orange and the carbon-rich biochar structure. The activation of biochar with sodium carbonate enhances its porosity, increasing the number of active sites and further improving its adsorption capacity. These interactions make Na_2CO_3 activated biochar an effective material for removing methyl orange from wastewater, highlighting its potential in environmental cleanup applications.

Conclusion

This study demonstrates the effectiveness of Na_2CO_3 activated puffed rice biochar in adsorbing MO dye from wastewater. Through FTIR, SEM and XRD analyses, the biochar's structural and chemical properties were thoroughly characterized, highlighting key features that enhance its adsorption capacity. FTIR analysis identified functional groups involved in the adsorption process, while SEM images revealed the porous structure of the biochar, which is essential for providing a large surface area for dye adsorption. The XRD analysis confirmed the amorphous nature of the biochar, supporting its ability to interact with organic molecules like MO.

Adsorption data, modeled using Langmuir and Freundlich isotherms, showed that the process follows the Langmuir model, indicating monolayer adsorption on a uniform surface. The adsorption capacity increased with higher Na_2CO_3 concentrations and larger amounts of biochar, with optimal results achieved at 4.0 mol/L Na_2CO_3 and 1.0 g of biochar.

The study also examined the effect of temperature on the adsorption process. Results indicated that adsorption is endothermic, with increasing temperatures leading to improved adsorption efficiency for both Na_2CO_3 concentrations (1.0 mol/L and 2.0 mol/L). The best adsorption performance was observed at 40 °C, where the interaction between biochar and MO was strongest, likely due to enhanced diffusion of MO molecules into the biochar's pores at higher temperatures.

In closing, Na_2CO_3 activated puffed rice biochar proves to be an efficient adsorbent for removing MO dye from wastewater. Its porous structure, active functional groups and favorable adsorption characteristics make it a promising material for dye removal and environmental remediation applications. The adsorption process is significantly influenced by temperature, with higher temperatures promoting more effective dye removal.

Conflict of Interest. The authors declare that they have no conflict of interest.

References

- Adithya, G., Rangabhashiyam, S., Sivasankari, C. 2019. Lanthanum-iron binary oxide nanoparticles: as cost effective fluoride adsorbent and oxygen gas sensor. *Microchemical Journal*, **148**: 364-373. <https://doi.org/10.1016/j.microc.2019.05.003>
- Anisuzzaman, S.M., Joseph, C., Daud, W.M.A.W., Krishnaiah, D., Sie Yee, H. 2015. Preparation and characterization of activated carbon from *Typha orientalis* leaves. *International Journal of Industrial Chemistry*, **6**: 9-21. <https://doi.org/10.1007/s40090-014-0027-3>
- Ayawei, N., Ebelegi, A.N., Wankasi, D. 2017. Modelling and interpretation of adsorption isotherms. *Journal of Chemistry*, **2017**: 1-11. <https://doi.org/10.1155/2017/3039817>
- Azizullah, A., Khattak, M.N.K., Richter, P., Häder, D.P. 2011. Water pollution in Pakistan and its impact on public health: a review. *Environment International*, **37**: 479-497. <https://doi.org/10.1016/j.envint.2010.10.007>
- Baker, F.S., Mitter, C.E., Repic, A.J., Tottes, E.D. 1992. Activated carbon. Kirk-Othmer *Encyclopedia of Chemical Technology*, **4**: 1015-1037.
- Balarak, D., Mahdavi, Y., Bazrafshan, E., Mahvi, A.H. 2016. Kinetic, isotherms and thermodynamic modeling for adsorption of acid blue 92 (AB92) from aqueous solution by modified *Azolla filiculoides*. *Fresenius Environmental Bulletin*, **25**: 1322-1331.
- Bangladesh Bureau of Statistics (BBS). 2017. *Statistical Yearbook of Bangladesh*, pp. 9-190, Statistics Division, Ministry of Planning, Government of the People's Republic of Bangladesh, Dhaka. <https://www.scirp.org/reference/referencespapers?referenceid=3115454>
- Bangladesh Bureau of Statistics (BBS). 2018. *Bangladesh Statistics 2018*, pp. 65-67, Statistics and Informatics Division (SID), Ministry of Planning, Government of the People's Republic of Bangladesh.
- Bazrafshan, E., Zarei, A.A., Nadi, H., Zazouli, M.A. 2014. Adsorptive removal of methyl orange and reactive red 198 dyes by *Moringa peregrina* ash. *Indian Journal of Chemical Technology*, **21**: 105-113.
- Cui, M.H., Cui, D., Gao, L., Cheng, H.Y., Wang, A.J. 2016. Analysis of electrode microbial communities in an up-flow bioelectro-chemical system treating azo dye wastewater. *Electrochimica Acta*, **220**: 252-257. <https://doi.org/10.1016/j.electacta.2016.10.121>
- Demirbas, E., Kobya, M., Konukman, A.E. 2008. Error analysis of equilibrium studies for the almond shell activated carbon adsorption of Cr(VI) from aqueous solutions. *Journal of Hazardous Materials*, **154**: 787-794. <https://doi.org/10.1016/j.jhazmat.2007.10.094>
- Deng, H., Yang, L., Tao, G., Dai, J. 2009. Preparation and characterization of activated carbon from cotton stalk by microwave-assisted chemical activation application in methylene blue adsorption from aqueous solution. *Journal of Hazardous Materials*, **166**: 1514-1521. <https://doi.org/10.1016/j.jhazmat.2008.12.080>
- Doke, K.M., Chavan, A., Nalawade, R., Khan, E.M. 2013. Kinetics and equilibrium isotherm for adsorption of basic blue 9 dye onto activated charcoal prepared from *Bhagar* seed husk. *Journal of Materials and Environmental Science*, **4**: 374-383.
- FAO. 2020. FAO Regional Office for Asia and the Pacific. Implementation of the Global Strategy in Bangladesh. <http://www.fao.org/asiapacific/perspectives/agricultural-statistics/global-strategy/results-in-the-region/bangladesh/en/> [Retrieved on: 22.11.2020]
- Gao, Q., Xu, J., Bu, X.-H. 2019. Recent advances about metal-organic frameworks in the removal of pollutants from wastewater. *Coordination Chemistry Reviews*, **378**: 17-31. <https://doi.org/10.1016/j.ccr.2018.03.015>
- Gunarathne, V., Rajapaksha, A.U., Vithanage, M., Alessi, D.S., Selvasembian, R., Naushad, M., Ok, Y.S. 2020. Hydrometallurgical processes for heavy metals recovery from industrial sludges. *Critical Reviews in Environmental Science and Technology*, **52**: 1022-1062. <https://doi.org/10.1080/10643389.2020.1847949>
- Haitham, K., Razak, S., Nawi, M.A. 2014. Kinetics and isotherm studies of methyl orange adsorption by a highly recyclable immobilized polyaniline on a glass plate. *Arabian Journal of Chemistry*, **150**: 1012. <https://doi.org/10.1016/j.arabjc.2014.10.010>
- Hassan, M., Naidu, R., Du, J., Liu, Y., Qi, F. 2020. Critical review of magnetic biosorbents: their preparation, application and regeneration for wastewater treatment. *Science of the Total Environment*, **702**: 134893. <https://doi.org/10.1016/j.scitotenv.2019.134893>

- Hussaro, K. 2014. Preparation of activated carbon from palm oil shell by chemical activation with Na₂CO₃ and ZnCl₂ as impregnated agents for H₂S adsorption. *American Journal of Environmental Sciences*, **10**: 336-346. <https://doi.org/10.3844/ajessp.2014>
- Iwuozor, K.O., Oyekunle, I.F., Oladunjoye, I.O., Ibitogbe, E.O., Olorunfemi, T.T. 2021. A review on the mitigation of heavy metals from aqueous solution using sugarcane bagasse. *Sugar Technology*, **24**: 1167-1185. <https://doi.org/10.1007/s12355-021-01051-w>
- Ji, Y., Li, T., Zhu, L., Wang, X., Lin, Q. 2007. Preparation of activated carbons by microwave heating KOH activation. *Applied Surface Science*, **254**: 506-512. <https://doi.org/10.1016/j.apsusc.2007.06.034>
- Jiang, T., Fang, W., Zhao, Q., Liu, W., Zhao, H., Le, S. 2017. Synthesis of Fe (Co or Ni) loaded mesoporous carbon composites and their adsorption behaviours for methyl orange. *Journal of Nanoscience and Nanotechnology*, **17**: 5261-5270. <https://doi.org/10.1166/jnn.2017.13820>
- Kareem, K. 2016. Removal and recovery of methylene blue dye from aqueous solution using *Avena fatua* seed husk. *Ibn Al-Haitham Journal for Pure and Applied Science*, **29**: 179-194. <https://www.iasj.net/iasj/article/122565>
- Li, Q., Li, Y., Ma, X., Du, Q., Sui, K., Wang, D., Wang, C., Li, H., Xia, Y. 2017. Filtration and adsorption properties of porous calcium alginate membrane for methylene blue removal from water. *Chemical Engineering Journal*, **316**: 623-630. <https://doi.org/10.1016/j.cej.2017.01.098>
- Mo, J.H., Lee, Y.H., Kim, J., Jeong, J.Y., Jegal, J. 2008. Treatment of dye aqueous solutions using nanofiltration polyamide composite membranes for the dye wastewater reuse. *Dyes and Pigments*, **76**: 429-434. <https://doi.org/10.1016/j.dyepig.2006.09.007>
- Mulugeta, M., Lelisa, B. 2014. Removal of methylene blue (Mb) dye from aqueous solution by bioadsorption onto untreated *Parthenium hysterophorous* weed. *Modern Chemistry and Applications*, **2**: 1000146.
- Ogemdi, I.K. 2019. Heavy metal concentration of aphrodisiac herbs locally sold in the southeastern region of Nigeria. *Pharmaceutical Science and Technology*, **3**: 22. <https://doi.org/10.11648/j.pst.20190301.13>
- Ozer, D., Dursun, G., Ozer, A. 2007. Methylene blue adsorption from aqueous solution by dehydrated peanut hull. *Journal of Hazardous Materials*, **144**: 171-179. <https://doi.org/10.1016/j.jhazmat.2006.09.092>
- Park, J.H., Choppala, G.K., Bolan, N.S., Chung, J.W., Chuasavathi, T. 2011. Biochar reduces the bioavailability and phytotoxicity of heavy metals. *Plant and Soil*, **348**: 439-451. <https://doi.org/10.1007/s11104-011-0948-y>
- Saleh, T.A., Gupta, V.K. 2012. Photo-catalyzed degradation of hazardous dye methyl orange by use of a composite catalyst consisting of multi-walled carbon nanotubes and titanium dioxide. *Journal of Colloid and Interface Science*, **371**: 101-106. <https://doi.org/10.1016/j.jcis.2011.12.038>
- Selvasembian, R., Gwenzi, W., Chaukura, N., Mthembu, S. 2021. Recent advances in the polyurethane-based adsorbents for the decontamination of hazardous wastewater pollutants. *Journal of Hazardous Materials*, **417**: 125960. <https://doi.org/10.1016/j.jhazmat.2021.125960>
- Seow, Y.X., Tan, Y.H., Mubarak, N.M., Kansedo, J., Khalid, M., Ibrahim, M.L., Ghasemi, M. 2022. A review on biochar production from different biomass wastes by recent carbonization technologies and its sustainable applications. *Journal of Environmental Chemical Engineering*, **10**: 107017. <https://doi.org/10.1016/j.jece.2021.107017>
- Socrates, G. 2004. *Infrared and Raman Characteristic Group Frequencies: Tables and Charts*, pp. 368, John Wiley & Sons, New York, USA.
- Thilagan, J., Gopalakrishnan, S., Kannadasan, T. 2013. Thermodynamic study on adsorption of copper (II) ions in aqueous solution by chitosan blended with cellulose & cross-linked by formaldehyde, chitosan immobilized on red soil, chitosan reinforced by banana stem fibre. *International Journal of Scientific Research Engineering and Technology*, **2**: 028-0036.
- Torrades, F. 2014. Using central composite experimental design to optimize the degradation of real dye wastewater by Fenton and Photo-Fenton reactions. *Dyes and Pigments*, **100**: 184-189. <https://doi.org/10.1016/j.dyepig.2013.09.004>
- Wang, L., Wang, Y., Ma, F., Tankpa, V., Bai, S., Guo, X., Wang, X. 2019. Mechanism and reutilization of modified biochar used for removal of heavy metals from wastewater: A review. *Science of the Total Environment*, **668**: 1298-1309. <https://doi.org/10.1016/j.scitotenv.2019.03.011>
- Yuan, P., Wang, J., Pan, Y., Shen, B., Wu, C. 2019.

- Review of biochar for the management of contaminated soil: preparation, application and prospect. *Science of The Total Environment*, **659**: 473-490. <https://doi.org/10.1016/j.scitotenv.2018.12.400>
- Zhang, L., Sellaoui, L., Franco, D., Dotto, G.L., Bajahzar, A., Belmabrouk, H., Bonilla-Petriciolet, A., Oliveira, M.L.S., Li, Z. 2020. Adsorption of dyes brilliant blue, sunset yellow and tartrazine from aqueous solution on chitosan: analytical interpretation via multilayer statistical physics model. *Chemical Engineering Journal*, **382**: 122592. <https://doi.org/10.1016/j.cej.2019.122952>
- Zhul-quarnain, A., Ogemdi, I.K., Modupe, I., Gold, E., Chidubem, E.E. 2018. Adsorption of malachite green dye using orange peel. *Journal of Biomaterials*, **2**: 36-42. <https://doi.org/10.11648/j.jb.20180202.12>